

Amorphous hydrogenated silicon-carbon-tin alloy films

F. Demichelis, G. Kaniadakis, A. Tagliaferro, and E. Tresso
Dipartimento di Fisica del Politecnico di Torino, I-10129 Torino, Italy

P. Rava

Elettrorava S.p.A., I-10040 Savonera (Torino), Italy

(Received 28 May 1987)

A new amorphous semiconductor alloy system α -Si-C-Sn:H has been prepared by rf magnetron sputtering of Sn in an atmosphere of SiH_4 , CH_4 , and Ar. Optical properties and dark conductivity of thin films are measured as a function of CH_4 flux. The dark conductivity displays a transition to a hopping-conduction mechanism as the CH_4 flux increases. In ir spectra, C-Sn and Sn-Sn vibrational bands are observed at 510 and 150 cm^{-1} , respectively. Dangling-bond density values are deduced from ESR measurements.

I. INTRODUCTION

The preparation and properties of amorphous carbon films and the effect of hydrogen were investigated by many authors.¹⁻⁴ Amorphous carbon can be considered as a two-phase system: one consisting of a structure rich in threefold-coordinated carbon and characterized by aromatic rings, the other of a structure rich in hydrogen containing predominantly saturated hydrocarbons. Amorphous carbon presents a low index of refraction, low extinction coefficient, and low optical gap when the graphitic structure prevails, and a large band gap when a diamondlike structure is predominant. Though α -C:H is a nonphotoconductive material, alloys of carbon with group-IV amorphous semiconductors are known to improve the optoelectronic properties of that element. Amorphous-carbon-based alloys are interesting because the group -IV elements are isoelectronic; they are not expected to increase the number of localized states⁵ or the activation energy. Amorphous semiconductors of this type also maintain local order with tetrahedral coordination, and therefore the band-structure properties are expected to remain similar to those of their crystalline counterpart.⁶

The amorphous hydrogenated silicon-carbon alloy is a classic example. The introduction into amorphous carbon of a controlled amount of silicon (>45%) (Ref. 7) limits the graphitic sp^2 bonds and yields a photoconductive material.^{8,9} Amorphous hydrogenated carbon-germanium alloys have also apparently been obtained.¹⁰ Recently a new alloy, amorphous hydrogenated carbon-tin, has been made and studied.^{11,12} This alloy shows attractive optical and electronic properties and constitutes a new material useful in photovoltaic devices. Another new alloy, amorphous silicon-tin, has an optical gap smaller than hydrogenated amorphous silicon and a high refractive index.^{6,13-16}

In this paper we report on a new amorphous carbon-based alloy: amorphous hydrogenated silicon-carbon-tin (α -Si-C-Sn:H). This alloy shows a very good transmittance, better than that of an α -Si-C:H alloy, optical gap

in the range 0.6 to 2.6 eV, depending on the amount of tin, low index of refraction, and relatively good dark conductivity.

Optical constants and optical gap were extracted from transmittance and reflectance measurements in the uv, visible, and near ir. Infrared spectra were recorded by absorption spectroscopy. The amount of tin in the alloy was determined from the integrated intensities of C-Sn vibration bands. ESR measurements provide information about the spin density of the samples.

II. EXPERIMENTAL

A. Film deposition

α -Si-C-Sn:H samples were deposited by plasma-assisted rf magnetron sputtering. A vacuum chamber of volume 37 l was evacuated by a 450- l s^{-1} turbomolecular pump. Two magnetron cathodes with Sn targets of 10 cm diameter (Sn purity 99.9995%) were placed in the top wall of the chamber, and substrates were placed on a rotating table on the bottom of the chamber. A mixture of SiH_4 , CH_4 , and Ar was introduced into the chamber controlling separately the flow of each gas. The pressure was kept constant at a desired value by adjusting the pumping speed by means of a throttle valve. Deposition of C, Si, and H originated from the decomposition of SiH_4 and CH_4 , and deposition of Sn originated from the sputtering of the Sn cathodes by Ar; rf power (13.56 MHz) was applied to the cathodes and a glow discharge was excited in the gas mixture. Deposition conditions of each sample are summarized in Table I. Each sample is labeled with the symbol GD followed by a number indicating ten times the CH_4 flux in sccm (standard cubic centimeters). The symbol I indicates the samples deposited for ir measurement.

B. Characterization of the films

The optical measurements were recorded on a Perkin-Elmer (uv visible near-ir) Lambda 9 spectrophotometer in the 0.2–1.5- μm wavelength range. Transmittance and

TABLE I. Deposition conditions for various samples.

Sample	$F(\text{SiH}_4)$ (sccm)	Gas Flux		Gas pressure P_t (Pa)	Power P_{rf} (W)	Voltage V_{dc} (V)	Time t (min)
		$F(\text{CH}_4)$ (sccm)	$F(\text{Ar})$ (sccm)				
GD 025	5	2.5	5	27	400	500	30
GD 050	5	5	5	27	400	380	30
GD 075	5	7.5	5	27	400		30
GD 100	5	10	5	27	400		30
GD 025-I	5	2.5	5	27	400	430–320	120
GD 050-I	5	5	5	27	400	400–340	120
GD 075-I	5	7.5	5	27	400	380–340	120
GD 100-I	5	10	5	27	400	440–280	120

reflectance measurements were performed on films deposited on a 2-mm-thick quartz substrate. The thickness of the films was measured by means of a Dektak II Stylus Profiler. The analysis yielding the index of refraction n , the extinction coefficient k , and hence the dielectric constant ϵ and the optical band gap from the transmittance, reflectance, and thickness measurements was based on a procedure whose details have been described in Refs. 17 and 18. The nature of chemical bonding between constituents was studied by ir spectroscopy in the absorption mode using a single-beam Perkin-Elmer 1710 Fourier spectrophotometer between 400 and 4000 cm^{-1} and a Bruker IFS 113 V between 100 and 400 cm^{-1} . All transmission measurements were made relative to uncoated silicon substrate as a reference.

ESR measurements were performed by means of a Varian EPR-109 spectrometer. Both the g values and the intensity of the spin-resonance signals of the samples were measured by comparison with the values obtained for DPPH (1,1-diphenyl-2-picrylhydrazyl, $g=2.0036$) and Varian pitch (KCl γ irradiated, $g=2.0029$) standard samples.

Resistances were measured, under vacuum which was maintained at about 10^{-2} Pa, with a Hewlett-Packard 4329 A high-resistance meter. Direct voltage in the

range from 10 to 250 V in direct and reverse bias was applied on Al electrodes ($4 \times 1 \text{ mm}^2$) pre-evaporated onto Corning glass substrate. The Ohmic behavior of the electrode contacts was checked at temperatures ranging between 20 and 250 $^\circ\text{C}$.

III. RESULTS AND DISCUSSION

A. Optical properties

Transmittance T and reflectance R spectra of typical samples, realized with different CH_4 gas pressure, are reported in Fig. 1. The refractive index n and the extinction coefficient k of the two samples as a function of the wavelength are reported in Fig. 2. The curves shown, and the other experimental results not reported in Fig. 2 because of the overlapping of the curves, indicate that the refractive indexes have low values and are practically independent of λ for all the films and undergo decreasing dispersion with increasing CH_4 flux. The extinction coefficient shows a pronounced decrease with CH_4 flux increase. Since the x-ray diffraction pattern of the samples show characteristic amorphous structure of the films, the optical gap was determined from the optical measurements using the methods applied to amorphous semiconductors.¹⁹

The optical gap E_g was obtained from the well-known expression

$$(\alpha E)^{1/2} = \gamma(E - E_g), \quad (1)$$

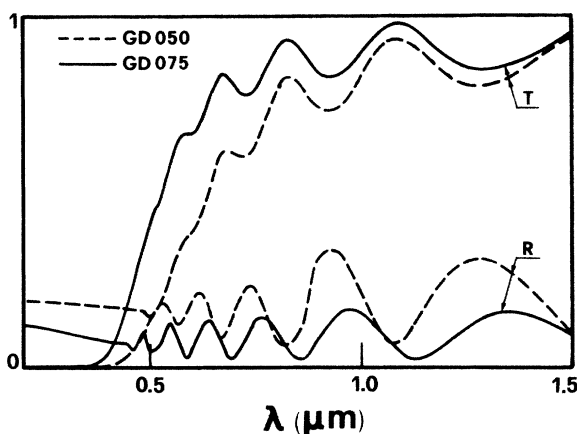


FIG. 1. Normalized transmittance and reflectance spectra for two samples with different CH_4 flux.

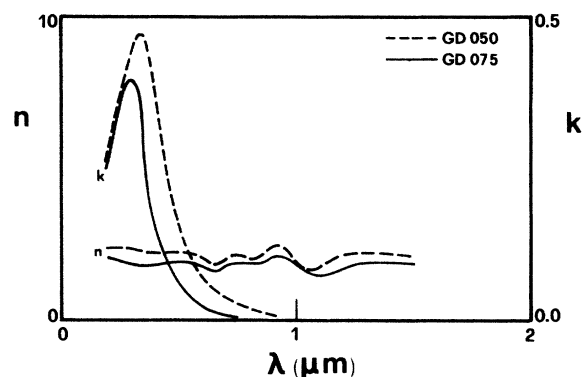


FIG. 2. Index of refraction n and extinction coefficient k for the samples of Fig. 1.

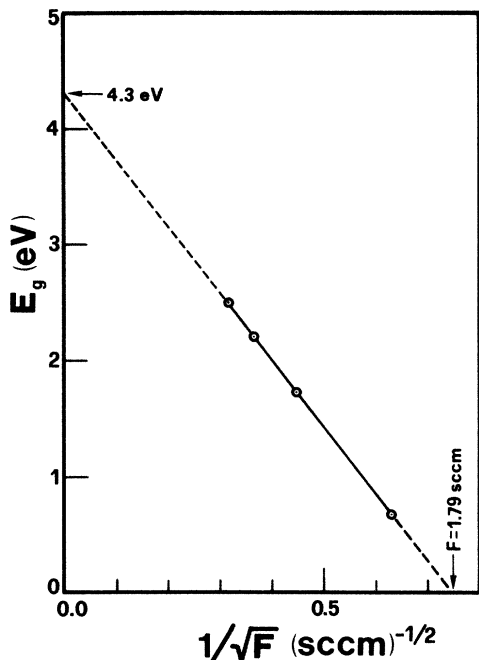


FIG. 3. CH₄ flux influence over energy-gap value.

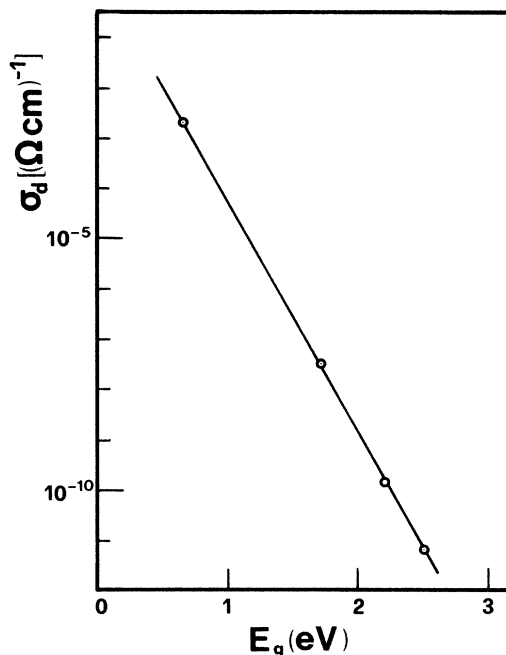


FIG. 4. Intrinsic conductivity behavior of *a*-Si-C-Sn:H samples.

where α is the absorption coefficient. Figure 3 shows the optical band gap E_g of *a*-Si-C-Sn:H alloys as a function of the inverse of the square root of the CH₄ flux. This trend indicates a threshold for semiconducting behavior for a given value of the CH₄ flux and an E_g value of ~ 4.3 eV from extrapolation of the straight line to the infinite flux. This is in agreement with the diamondlike-structure optical band gap, as it is expected for very high CH₄ flux.

B. Electrical properties

Figure 4 shows the room-temperature dark conductivity σ_d of the films as a function of optical band gap E_g . The linearity of this plot suggests an intrinsic conductivity behavior of the material and provides a value of σ_0 , obtained by extrapolation to $E_g = 0$, of $\sim 130 \text{ } \Omega^{-1} \text{ cm}^{-1}$, similar to the value of minimum metallic conductivity ($200 \text{ } \Omega^{-1} \text{ cm}^{-1}$) given by Mott.²⁰

In Fig. 5(a) is reported the trend of $\log_{10} \sigma_d$ versus $1000/T$ for the sample GD025. The slope of $\log_{10} \sigma_d$ shows activated conductivity behavior for samples with low CH₄ flux, indicating conduction by extended states. When the CH₄ flux increases the mechanism changes to hopping since the σ_d plot exhibits a curvature while the slope of $\log_{10} \sigma_d$ versus $(1/T)^{1/4}$ shows a linear trend, as shown in Fig. 5(b) (sample GD050).

C. Electron-spin resonance

ESR signals for our *a*-Si-C-Sn:H films are very sensitive to CH₄ flux (Sn content). ESR spectra for three

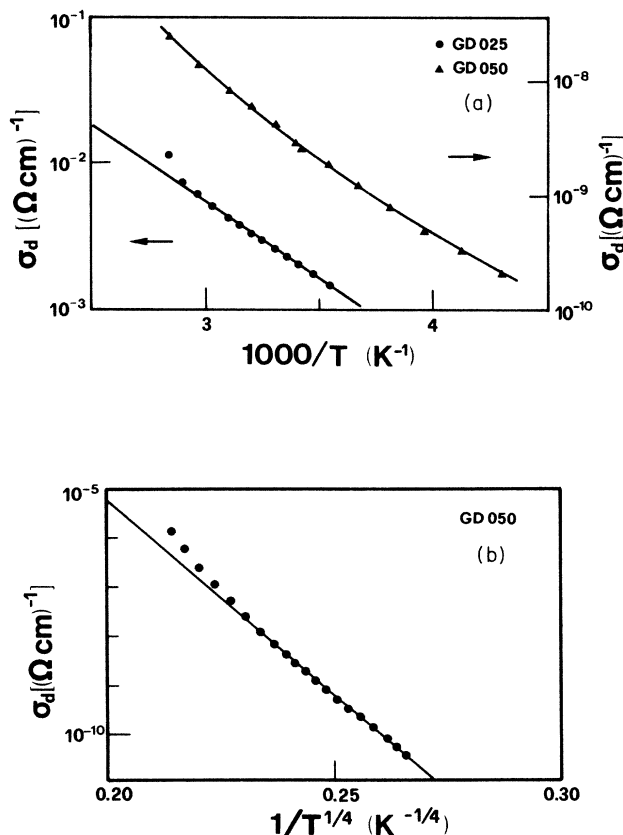


FIG. 5. Conductivity behavior: (a) activated for GD025, (b) hopping for GD050.

films are shown in Fig. 6. As CH_4 flux increases the signal related to C dangling bonds rapidly increases (see Table II).

We obtain for carbon a value of $g=2.0034$, greater than that of amorphous carbon. This fact could indicate a higher localization of the paramagnetic states with respect to that of hydrogenated amorphous carbon. The density of states is comparable with that of the annealed $\alpha\text{-Si:H}$ samples and decreases when CH_4 flux decreases. The large value of the linewidth (peak to peak) of 1.3×10^{-3} T for C dangling bonds indicates a complex structure of the signal due to the presence of different elements.

IV. BONDING AND STRUCTURE

A. ir spectroscopy

The general trend of ir absorption spectra between 400 and 4000 cm^{-1} is similar to those observed by many authors on amorphous carbon^{2,7,21,22} and hydrogenated amorphous silicon-carbon alloys.^{7,10,23,24} Two typical ir transmission spectra of two different samples are shown in Fig. 7. The peaks of the various CH_2 , CH_3 , SiH, and SiC vibration modes are present, while the absorption band at 510 cm^{-1} is consistent with the presence of an organotin phase around the Sn—C bonding. In the range $100\text{--}400 \text{ cm}^{-1}$ a peak at 150 cm^{-1} present in samples rich in Sn content is consistent with Sn—Sn bonding. The integrated intensities contributing to a specific vibration mode are evaluated using the expression

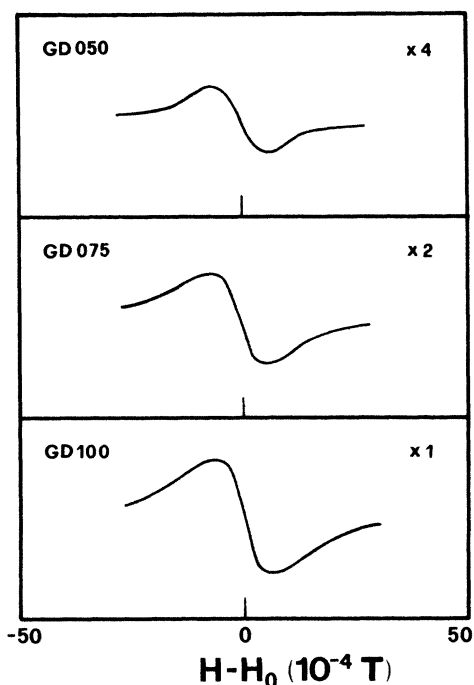


FIG. 6. ESR spectra for samples with different CH_4 flux. Magnification shown on each plot, H_0 is the magnetic field corresponding to the resonance.

TABLE II. ESR signals for samples prepared with different CH_4 fluxes. I , relative intensity; v , volume of the film; ΔH_{pp} , linewidth peak to peak.

Sample	g	ΔH_{pp} (T)	I/v (a.u.)	Dangling bonds (cm^{-3})
GD 025				
GD 050	2.0033	1.3×10^{-3}	400.253	9.4×10^{19}
GD 075	2.0034	1.3×10^{-3}	989.701	2.3×10^{20}
GD 100	2.0034	1.2×10^{-3}	2048.338	4.8×10^{20}

$$S = \int \frac{\alpha(\omega)}{\omega} d\omega, \quad (2)$$

where $\alpha(\omega)$ is the absorption coefficient for frequency ω and the integration is over the deconvoluted absorption peak corresponding to the respective vibration mode. The number of oscillators for unit volume N can be given by the expression reported by Brodsky *et al.*,²⁵

$$N = \frac{(1+2\epsilon)^2}{9\epsilon^2} e^{1/2} \frac{N_A}{\Gamma/\zeta} \int \frac{\alpha(\omega)}{\omega} d\omega \quad (3)$$

or by the expression given by Connell and Pawlik²⁶

$$N = \frac{9\epsilon^{1/2}}{(\epsilon+2)^2} \frac{N_A}{\Gamma/\zeta} \int \frac{\alpha(\omega)}{\omega} d\omega. \quad (4)$$

In Eqs. (3) and (4) we take values of ϵ corresponding to the values of the index of refraction n included in the range of our experimental values, N_A is the Avogadro number, and Γ/ζ the integrated strength of the corresponding band in a gaseous hydride. The content of tin was obtained considering the Sn—Sn bond at 150 cm^{-1} and the C—Sn bond at 510 cm^{-1} . We obtain values of $N = 5.5 \times 10^{21} \text{ cm}^{-3}$ and $N = 7.5 \times 10^{20} \text{ cm}^{-3}$ for the two samples GD 025 and GD 050.

The integrated intensities of C—H (2900 cm^{-1}), Si—H (2100 cm^{-1}), and Si— CH_3 (1250 cm^{-1}) vibration modes obtained as a function of CH_4 flux are shown in Fig. 8.

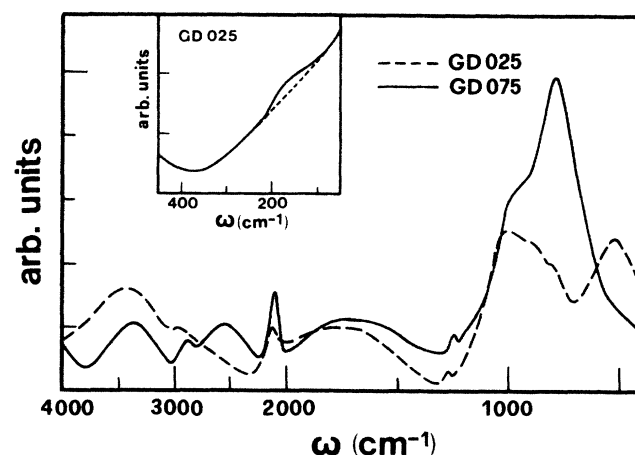


FIG. 7. ir absorption spectra for two samples with different CH_4 flux.

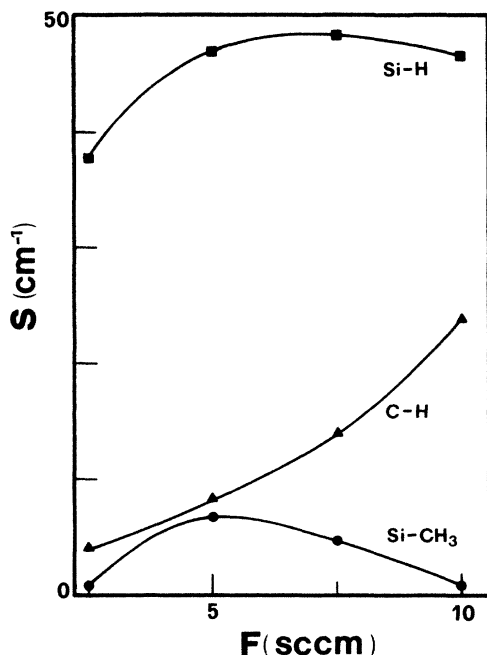


FIG. 8. Integrated intensities of C-H (2900 cm^{-1}), Si-H (2100 cm^{-1}), and Si-CH₃ (1250 cm^{-1}) vibration modes as a function of CH₄ flux.

One observes that when CH₄ flux increases the C-H contribution sensibly increases, while the Si-H show after a slight increase, a trend that is about constant, and the Si-CH₃ reach a maximum and after decrease.

For low CH₄ flux the sputtering seems to be predominant since the C-Sn and Sn-Sn vibrational modes are present only for low CH₄ flux. For high CH₄ flux the glow discharge of SiH₄ and CH₄ takes place, giving depositions having a structure rich in C-H bonds. Furthermore, our results seem to confirm the preferential attachment of H to C or Si rather than Sn bonding sites.

V. CONCLUSIONS

Amorphous hydrogenated carbon-tin-silicon alloys prepared by rf magnetron sputtering have been investigated and the following conclusions obtained

(1) The index of refraction is low and practically independent of the wavelength; the optical gap decreases as the CH₄ flux decreases and the films do not show semiconducting properties when the CH₄ flux lowers a given threshold.

(2) In ir spectra 510- and 150-cm^{-1} bands are identified with C-Sn and Sn-Sn vibrational bands, respectively. The integrated intensities give the tin content. The bands of the different C-Si, Si-H, and C-H bonds are also identified; their integrated intensities determined as a function of CH₄ flux indicate the presence of C-Sn and Sn-Sn bonds in the films deposited at low flux and a remarkable increase of C-H bonds as the CH₄ flux increases while the Si-H contribution remains practically constant.

(3) The dark conductivity increases as CH₄ flux increases. Our results suggest a transition from activated conductivity to hopping conductivity behavior with increasing CH₄ flux.

In conclusion, we can deduce that the presence of carbon in an Si-Sn alloy and a convenient tin content allow us to obtain an amorphous alloy showing good optical and electrical properties.

ACKNOWLEDGMENTS

This research was supported in part by grants from the Research Project PFE2 sponsored by Consiglio Nazionale delle Ricerche. The authors are grateful to SIO Bugas Airliquide for kindly providing the gases and the gas-handling equipment used in the deposition. The authors would like to thank Professor E. Giamello and Dr. M. Fanciulli for their collaboration in ESR measurements. G. Kaniadakis wishes to thank the International Centre for Theoretical Physics, Trieste, for providing a grant.

¹S. K. Das, M. Kaminsky, L. H. Rovner, J. Chin, and K. Y. Chen, *Thin Solid Films* **63**, 227 (1979).

²D. R. McKenzie, R. C. McPhedran, N. Savvides, and D. J. H. Cochagne, *Thin Solid Films* **108**, 247 (1983).

³F. H. Smith, *J. Appl. Phys.* **55**, 764 (1984).

⁴F. Demichelis, M. Fanciulli, G. Kaniadakis, A. Tagliaferro, E. Tresso, P. Rava, and E. Giamello, *Proceedings of the European MRS Conference, Strasbourg* (Editiones de Physique, Paris, 1982).

⁵J. J. Hauser, *J. Non-Cryst. Solids* **23**, 21 (1977).

⁶C. Vérié, J. F. Rochette, and J. P. Rebouillet, *J. Phys. (Paris) Colloq.* **10**, C4-667 (1981).

⁷H. Wieder, M. Cardona, and C. R. Guarnieri, *Phys. Status Solidi* **92**, 99 (1979).

⁸T. Shimada, Y. Katayama, and K. F. Komatsubara, *J. Appl. Phys.* **50**, 5530 (1979).

⁹Y. Tawada, M. Kondo, H. Okamoto, and Y. Hamakawa, *Solar Energy Mater.* **6**, 299 (1982).

¹⁰Y. Catherine and G. Turban, *Thin Solid Films* **70**, 101 (1980).

¹¹P. Mpawenayo, F. Demichelis, P. Rava, A. Tagliaferro, E. Tresso, and G. Kaniadakis, *Thin Solid Films* **146**, L19 (1987).

¹²F. Demichelis, G. Kaniadakis, P. Mpawenayo, M. A. Perino, A. Tagliaferro, E. Tresso, P. Rava, G. Della Mea, and M. Vallino, *Thin Solid Films* **150**, 189 (1982).

¹³D. L. Williamson and S. K. Deb, *J. Appl. Phys.* **54**, 2588 (1983).

¹⁴H. Itozaki, N. Fujita, T. Igarashi, and H. Hitotouyanagi, *J. Non-Cryst. Solids* **59-60**, 589 (1983).

¹⁵A. H. Mahan, D. L. Williamson, and A. Madan, *Appl. Phys. Lett.* **44**, 220 (1984).

¹⁶G. N. Pursons, J. W. Cook, Jr., G. Lucovsky, S. Y. Lin, and M. J. Martin, *J. Vac. Sci. Technol. A* **4**, 470 (1986).

¹⁷F. Demichelis, E. Minetti-Mezzetti, A. Tagliaferro, and E. Tresso, *Nuovo Cimento* **4D**, 68 (1984).

¹⁸F. Demichelis, G. Kaniadakis, A. Tagliaferro, and E. Tresso,

- Appl. Opt. **26**, 1757 (1987).
- ¹⁹G. D. Cody, B. G. Brooks, and B. Abeles, *Sol. Energy Mater.* **8**, 231 (1982).
- ²⁰N. F. Mott, *Philos. Mag.* **22**, 7 (1970).
- ²¹B. Discheler, A. Bubenzer, and P. Koidl, *Appl. Phys. Lett.* **42**, 636 (1983).
- ²²A. H. Mahan, B. Von Roedern, D. L. Williamson, and A. Madan, *J. Appl. Phys.* **57**, 2717 (1985).
- ²³S. Morimoto, T. Miura, M. Kumedas, and T. Shimizu, *Jpn. J. Appl. Phys.* **21**, L219 (1982).
- ²⁴F. Demichelis, G. Kaniadakis, E. Mezzetti, P. Mpawenayo, A. Tagliaferro, E. Tresso, P. Rava, and G. Della Mea, *Nuovo Cimento* **9**, 4 (1987).
- ²⁵M. H. Brodsky, M. Cardona, and J. J. Cuomo, *Phys. Rev. B* **16**, 3556 (1977).
- ²⁶G. A. N. Connell and J. R. Pawlik, *Phys. Rev. B* **13**, 787 (1976).